Igor Pažanin* and Marko Radulović

On the Heat Flow Through a Porous Tube Filled with Incompressible Viscous Fluid

https://doi.org/10.1515/zna-2019-0350 Received November 25, 2019; accepted February 17, 2020; previously published online March 17, 2020

Abstract: We studied the non-isothermal flow of an incompressible viscous fluid through a porous tube. Motivated by filtration problems, Darcy's law was incorporated on the walls of the tube and the flow was pressure driven. The main goal was to investigate the thermodynamic part of the system, assuming that the hydrodynamic part is known. In view of the applications we wanted to model, the fluid inside the tube was supposed to be cooled (or heated) by the surrounding medium. Using asymptotic analysis with respect to the small parameter (being the ratio between the tube's thickness and its length), we constructed the explicit second-order approximation for the temperature distribution of the fluid. Numerical examples are provided to compare the obtained solution with the one derived for a rigid tube and also to show the corrections due to higher-order terms.

Keywords: Asymptotic Approximation; Darcy's Law; Heat Flow; Numerical Examples; Porous Tube.

1 Introduction

Pressure-driven flows through cylindrical domains with porous walls have raised considerable interest due to their practical significance. Such flows appear in numerous applications with filtration systems incorporated, namely in industrial devices for irrigation, medical devices for artificial kidney analysis, transpiration cooling systems, etc. In those systems, the filtration process naturally occurs when fluid is pumped axially through a tubular membrane, forcing the purified filtrate to exit through the membrane while the concentrate exits downstream. Fluid flow in porous tubes has been extensively studied by many

researchers, mostly in isothermal regimes where temperature variations of the fluid have been neglected. The goal of the present study was to investigate the non-isothermal flow, i.e. to explore the behaviour of the fluid temperature, in a porous tubular membrane.

Dealing with non-isothermal flows in a tube with porous walls is very challenging from the analytical point of view. The problem is described by a complex non-linear system of partial differential equations in which Navier-Stokes equations are coupled with heat conduction equations. Moreover, coupling between the transmembrane pressure and the velocity should also be taken into consideration. If one aims to analytically address such flows, certain decoupling in the original system must take place. In view of that, in the present paper we are going to consider only the thermodynamic part of the system, assuming that the velocity distribution is known and given by the solution proposed by Tilton et al. [1]. This means that the governing problem is described by the non-steady heat equation with a given velocity in the convection term (see Section 2). To be in line with the above-mentioned applications, we assume that the tube is plunged in the medium whose temperature differs from the fluid temperature inside the tube. We describe this particular heat exchange process by the Newton cooling condition prescribed on the permeable walls of the tube. A small parameter ε is naturally introduced into the problem, denoting the ratio between the tube's thickness and its length. Considering the flow in a tube, which is either very thin or very long, is reasonable from the point of view of the applications and allows us to perform asymptotic analysis with respect to ε . There are a number of papers concerning the derivation of asymptotic models for fluid flows through a tube with rigid walls. An asymptotic model for the heat flow through a thin cooled pipe filled with a micropolar fluid has been derived in [2]. The effects of strong convection on the cooling process for a long or thin pipe were considered in [3] and [4], respectively, where the corresponding asymptotic models have been rigorously derived and justified. Finally, the rigorous derivation of the models for the heat transfer in a laminar flow through a helical and a distorted pipe has been provided in [5] and [6], respectively. Therefore, starting from the non-dimensional setting and employing the approach we developed for fluid flows through tubes with rigid walls in the papers mentioned above, we

Marko Radulović: Department of Mathematics, Faculty of Science, University of Zagreb, Bijenička 30, 10000 Zagreb, Croatia, E-mail: mradul@math.hr

^{*}Corresponding author: Igor Pažanin, Department of Mathematics, Faculty of Science, University of Zagreb, Bijenička 30, 10000 Zagreb, Croatia, E-mail: pazanin@math.hr

managed to derive a second-order approximation for the temperature distribution via a two-scale expansion technique (see Section 3). Being in explicit form, the solution indicates how the exterior temperature and the coupling between the transmembrane pressure and velocity affect the heat flow inside the tube. Those effects can be clearly visualised as shown in Section 4 containing the numerical examples.

To the best of our knowledge, analytical results have been reported only for isothermal regimes in which temperature variations of the fluid inside the tube are not taken into account. The pioneer results were from Berman [7] and Regirer [8]. Thereafter, one can find many papers addressing isothermal flows; we refer the reader to [1, 9– 16]. Allow us to emphasise the paper by Tilton et al. [1], which directly inspired the current study. In [1], Darcy's law, $u = \frac{k_m}{uh}p$, has been incorporated on the permeable surface, and, for the first time, the higher-order corrections in the asymptotic solution for the velocity are reported. Here, k_m stands for the membrane permeability, h denotes the membrane thickness, and μ the dynamic viscosity of the fluid. For the reader's convenience, we recover this solution in Appendix and use it as the entering velocity in our heat conduction problem. Concerning the nonisothermal regimes of the flow, in the existing literature one can find only the results based on experiments or numerical simulations (see, e.g. [17–23]). In view of that, this is the first attempt to analytically address the heat transfer in porous tubes and obtain explicit formulae for the solution, which represents our main contribution. We strongly believe that the proposed explicit approximation for the temperature distribution could prove useful in realworld applications, primarily in the design and optimisation of filtration systems naturally appearing in industrial devices for irrigation, medical devices for artificial kidney analysis, transpiration cooling systems, etc.

2 The Governing Problem

We consider the flow of an incompressible viscous fluid in a circular tube Ω with permeable walls, length L, and radius R (see Fig. 1). We introduce the small parameter as the ratio $\varepsilon = \frac{R}{L}$ implying that the considered tube is either very thin or very long. Next, we take into account the heat exchange between the surrounding medium and the fluid inside the tube by prescribing Newton's cooling condition on the lateral boundary. Supposing the flow is axisymmetric, our aim was to study the heat flow in Ω , assuming that the fluid velocity is known. In view of that, we address the

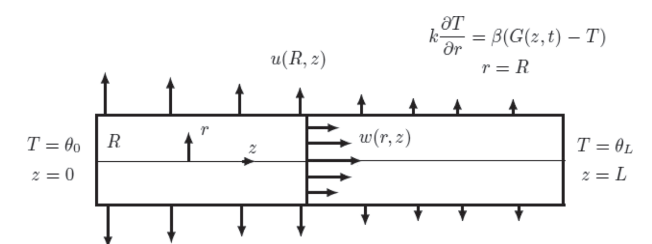


Figure 1: Flow configuration.

following non-steady convection–diffusion problem in Ω :

$$\rho C_p \left(\frac{\partial T}{\partial t} + u \frac{\partial T}{\partial r} + w \frac{\partial T}{\partial z} \right) = k \left(\frac{\partial^2 T}{\partial r^2} + \frac{1}{r} \frac{\partial T}{\partial r} + \frac{\partial^2 T}{\partial z^2} \right), \tag{1}$$

$$k\frac{\partial T}{\partial r} = \beta(G(z, t) - T)$$
 for $r = R$. (2)

Here, T(r, z, t) is the unknown fluid temperature, ρ is the fluid density, while C_p , k, and β are the positive constants denoting the specific heat capacity at constant pressure, the thermal conductivity, and the heat transfer coefficient, respectively. We assume that the axial w(r, z) and radial u(r, z) components of the velocity field are known in the system and given by the solution derived in [1] (see Appendix).

As mentioned above, in order to describe the cooling and heating process at the lateral boundary of the circular tube, we employ the well-known Newton's cooling law. The exterior temperature G(z,t) is assumed to be known in the Robin boundary condition (2), and its relation to the temperature of the fluid determines whether the process of heating or cooling will take place. Finally, we prescribe temperatures at the ends of the tube:

$$T = \theta_i(t) \quad \text{for } z = i, \ i = 0, L, \tag{3}$$

and impose the initial condition $T(r, z, 0) = T^0(r, z)$. The prescribing of the temperature at the ends of the tube is mathematically justified, as it leads to a closure of the governing problem. Due to the fact that the velocity field enters into the problem as a known function, the considered problem is linear, so the existence and uniqueness of results can be deduced via standard techniques (see, e.g. [24]). Still, there is no hope to derive the exact solution; thus, in the sequel, we want to construct the higher-order asymptotic approximation for temperature distribution.

As usual, we shall work in a non-dimensional setting. In view of that, we introduce the non-dimensionalised space variables

$$\hat{z}=rac{z}{L},\quad \hat{r}=rac{r}{R},$$

whereas the time is rescaled as

$$\hat{t} = \frac{k}{L^2 C_p \rho} t = \frac{\varepsilon^2 k}{R^2 C_p \rho} t.$$

Correspondingly, the functions in non-dimensional form are given by

$$\hat{u} = \frac{u}{\varepsilon \overline{w}_0}, \quad \hat{w} = \frac{w}{\overline{w}_0}, \quad \hat{T} = \frac{T}{T_{\text{ref}}},$$

where

$$\overline{w}_0 = \frac{1}{\pi R^2} \int\limits_0^R 2\pi w r \mathrm{d}r = \frac{2}{R^2} \int\limits_0^R w r \mathrm{d}r,$$

is the mean axial velocity at z=0 and $T_{\rm ref}$ denotes the characteristic temperature. We also introduce the Reynolds and Prandtl numbers as

$$Re = \frac{2R\overline{w}_0}{v}, \quad Pr = \frac{\rho v C_p}{k},$$
 (4)

with $v = \frac{\mu}{\rho}$ being the kinematic viscosity.

It is important to emphasise at this point that, in view of the applications, the typical range for the Reynolds number is from 10^2 for a laminar flow up to 10^6 for a turbulent flow, while the range of the Prandtl number is from 10^{-2} for mercury up to 10^5 for polymer melts. In order to be consistent with the work presented in [1], the illustrations in Section 4 have been presented for fixed Reynolds number equal to 150 and Prandtl number equal to 4.8.

We now obtain from (1), after multiplying with $\frac{R^2}{k}$, the following:

$$\varepsilon^{2} \frac{\partial \hat{T}}{\partial \hat{t}} + \frac{\varepsilon \rho C_{p} R \overline{w}_{0}}{k} \hat{u} \frac{\partial \hat{T}}{\partial \hat{r}} + \frac{\rho C_{p} R^{2} \overline{w}_{0}}{kL} \hat{w} \frac{\partial \hat{T}}{\partial \hat{z}}$$

$$= \frac{\partial^{2} \hat{T}}{\partial \hat{r}^{2}} + \frac{1}{\hat{r}} \frac{\partial \hat{T}}{\partial \hat{r}} + \varepsilon^{2} \frac{\partial^{2} \hat{T}}{\partial \hat{z}^{2}}.$$

Taking into account (4), we rewrite the above equation in the following way:

$$\varepsilon^{2} \frac{\partial \hat{T}}{\partial \hat{t}} + \frac{\varepsilon \operatorname{PrRe}}{2} \left(\hat{u} \frac{\partial \hat{T}}{\partial \hat{r}} + \hat{w} \frac{\partial \hat{T}}{\partial \hat{z}} \right)$$

$$= \frac{\partial^{2} \hat{T}}{\partial \hat{r}^{2}} + \frac{1}{\hat{r}} \frac{\partial \hat{T}}{\partial \hat{r}} + \varepsilon^{2} \frac{\partial^{2} \hat{T}}{\partial \hat{z}^{2}}.$$
(5)

Similarly, Newton's cooling condition (2) can be written in non-dimensional form as

$$\frac{\partial \hat{T}}{\partial \hat{r}} = \varepsilon N u(\hat{G}(\hat{z}, \hat{t}) - \hat{T}) \quad \text{for} \quad \hat{r} = 1.$$
 (6)

Here, $\hat{G} = \frac{G}{T_{tot}}$, while $Nu = \beta Lk^{-1}$ stands for the Nusselt number. The Nusselt number typically ranges from 1 to 10 for a laminar flow, while for a turbulent flow the ranges are usually from 10² to 10³. Again, in order to be consistent with the work provided in [1], we present the illustration in Section 4 for a fixed Nusselt number 4.8.

3 Asymptotic Analysis

We expand the temperature \hat{T} in powers of ε in the following way:

$$\hat{T}(\hat{z},\hat{r},\hat{t}) = \hat{T}_0(\hat{z},\hat{r},\hat{t}) + \varepsilon \hat{T}_1(\hat{z},\hat{r},\hat{t})$$

$$+ \varepsilon^2 \hat{T}_2(\hat{z},\hat{r},\hat{t}) + \cdots .$$
(7)

Substituting the expansion (7) into the systems (5) and (6) and collecting the zero-order terms, we obtain

1:
$$\frac{\partial^2 \hat{T}_0}{\partial \hat{r}^2} + \frac{1}{\hat{r}} \frac{\partial \hat{T}_0}{\partial \hat{r}} = 0$$
,

1:
$$\frac{\partial \hat{T}_0}{\partial \hat{r}} = 0$$
 for $\hat{r} = 1$.

We conclude that \hat{T}_0 is independent of \hat{r} , i.e. $\hat{T}_0 =$ $\hat{T}_0(\hat{z},\hat{t})$. This means that the heat flow is mostly in the axial direction, which was to be expected. Nevertheless, we continue the computation and seek for the higher-order terms. The $\mathfrak{O}(\varepsilon)$ terms yield the problem for the first-order corrector \hat{T}_1 :

$$\varepsilon: \frac{\partial^2 \hat{T}_1}{\partial \hat{r}^2} + \frac{1}{\hat{r}} \frac{\partial \hat{T}_1}{\partial \hat{r}} = \frac{\text{PrRe}}{2} \hat{w}_0 \frac{\partial \hat{T}_0}{\partial \hat{z}},$$

$$\varepsilon: \frac{\partial \hat{T}_1}{\partial \hat{r}} = Nu(\hat{G} - \hat{T}_0) \text{ for } \hat{r} = 1,$$
(8)

where $\hat{w}_0 = -\frac{1}{4}(1-\hat{r}^2)\frac{\partial \hat{p}_0}{\partial \hat{z}}$ is the zero-order approximation for the axial velocity. Here, the zero-order approximation for the pressure is given by $\hat{p}_0(z) = -2 \sinh(4\hat{z}) + 2 \sinh(4\hat{z})$ \hat{P}_{tm} cosh(4 \hat{z}), with \hat{P}_{tm} being the non-dimensional transmembrane pressure at $\hat{z} = 0$ (see Appendix).

The compatibility condition ensuring the existence of the solution to problem (8) gives

$$\left(-\int_{0}^{1}\frac{1}{4}(1-\hat{r}^{2})\hat{r}d\hat{r}\right)\frac{\Pr \operatorname{Re}}{2}\frac{\partial\hat{p}_{0}}{\partial\hat{z}}\frac{\partial\hat{T}_{0}}{\hat{z}}=Nu(\hat{G}-\hat{T}_{0}).$$

After simple integration, we obtain

$$-\frac{\text{PrRe}}{2}\frac{\partial \hat{p}_0}{\partial \hat{z}}\frac{\partial \hat{T}_0}{\partial \hat{z}} = 16Nu(\hat{G} - \hat{T}_0), \tag{9}$$

leading to

$$\frac{\partial \hat{T}_0}{\partial \hat{z}} = -\frac{32Nu(\hat{G} - \hat{T}_0)}{\text{PrRe}\frac{\partial \hat{p}_0}{\partial \hat{z}}}.$$

In view of that, the system (8) becomes

$$\frac{\partial^2 \hat{T}_1}{\partial \hat{r}^2} + \frac{1}{\hat{r}} \frac{\partial \hat{T}_1}{\partial \hat{r}} = 4(1 - \hat{r}^2) N u (\hat{G} - \hat{T}_0),$$

$$\frac{\partial \hat{T}_1}{\partial \hat{r}} = N u (\hat{G} - \hat{T}_0) \text{ for } \hat{r} = 1.$$

It can be solved by taking

$$\hat{T}_1(\hat{z},\hat{r},\hat{t}) = \left(\hat{r}^2 - \frac{\hat{r}^4}{4}\right) Nu(\hat{G} - \hat{T}_0) + \hat{C}(\hat{z},\hat{t}),$$
 (10)

where $\hat{C}(\hat{z}, \hat{t})$ is an unknown function, which we determine later from the compatibility condition related to the system for the second-order corrector \hat{T}_2 .

Let us now solve (9). Applying the expression for the pressure

$$\hat{p}_0(\hat{z}) = -2\sinh(4\hat{z}) + \hat{P}_{tm}\cosh(4\hat{z}),\tag{11}$$

into (9), we get

$$\begin{split} \frac{\partial \hat{T}_{0}}{\partial \hat{z}} &- \frac{16Nu}{\text{PrRe}(\hat{P}_{tm}-2)} \frac{e^{4\hat{z}}}{e^{8\hat{z}} - \frac{\hat{P}_{tm}+2}{\hat{P}_{tm}-2}} \hat{T}_{0} \\ &= - \frac{16Nu}{\text{PrRe}(\hat{P}_{tm}-2)} \frac{e^{4\hat{z}}}{e^{8\hat{z}} - \frac{\hat{P}_{tm}+2}{\hat{P}_{tm}-2}} \hat{G}(\hat{z},\hat{t}). \end{split}$$

For fixed $\hat{t} \in (0, 1)$, the above equation can be viewed as an ordinary differential equation (ODE) for \hat{T}_0 with respect to $\hat{z} \in (0, 1)$. Thus, the solution reads:

$$\hat{T}_0(\hat{z},\hat{t})$$

$$= A(t) \left(\frac{e^{4\hat{z}} - \sqrt{\frac{\hat{p}_{tm} + 2}{\hat{p}_{tm} - 2}}}{e^{4\hat{z}} + \sqrt{\frac{\hat{p}_{tm} + 2}{\hat{p}_{tm} - 2}}} \right)^{\frac{2Nu}{\Pr{Re}(\hat{P}_{tm} - 2)}} \sqrt{\frac{\hat{p}_{tm} + 2}{\hat{p}_{tm} - 2}}$$

$$- \left(\frac{e^{4\hat{z}} - \sqrt{\frac{\hat{p}_{tm} + 2}{\hat{p}_{tm} - 2}}}{e^{4\hat{z}} + \sqrt{\frac{\hat{p}_{tm} + 2}{\hat{p}_{tm} - 2}}} \right)^{\frac{2Nu}{\Pr{Re}(\hat{P}_{tm} - 2)}} \sqrt{\frac{1}{\hat{p}_{tm} + 2}}$$

$$\hat{z} \frac{16Nu}{\Pr{Re}(\hat{P}_{tm} - 2)} \hat{G}(\xi, \hat{t}) e^{4\xi} \left(\frac{e^{4\xi} - \sqrt{\frac{\hat{p}_{tm} + 2}{\hat{p}_{tm} - 2}}}{e^{4\xi} + \sqrt{\frac{\hat{p}_{tm} + 2}{\hat{p}_{tm} - 2}}} \right)^{-\frac{2Nu}{\Pr{Re}(\hat{P}_{tm} - 2)}} \sqrt{\frac{\hat{p}_{tm} + 2}{\hat{p}_{tm} - 2}}$$

$$\int_{0}^{2\pi} \frac{e^{8\xi} - \frac{\hat{p}_{tm} + 2}{\hat{p}_{tm} + 2}} (12)$$

To determine A(t), we need only one boundary condition, as (9) is a first-order equation. From the physical point of view, the natural choice is $\hat{T}_0(0,t) = \hat{\theta}_0(t)$, where $\hat{\theta}_0 = \frac{\theta_0}{T_{\rm ref}}$ [see (3)]. Indeed, the temperature of the fluid leaving the tube should not be known in advance. Consequently, we obtain

$$A(t) = \hat{\theta}_0 \left(\frac{1 + \sqrt{\frac{\hat{p}_{tm} + 2}{\hat{p}_{tm} - 2}}}{1 - \sqrt{\frac{\hat{p}_{tm} + 2}{\hat{p}_{tm} - 2}}} \right)^{\frac{2Nu}{\text{PrRe}(\hat{P}_{tm} - 2)} \sqrt{\frac{1}{\hat{p}_{tm} + 2}}}.$$
 (13)

We note at this point that the comparison of the expressions for the zero-order temperature approximation [see (12) and (13)] derived for the porous tube with the zero-order temperature approximation for the rigid tube given by (18) will be discussed and numerically illustrated in Section 4 (see also [2] for the expressions for the zero-order temperature approximation in a thin circular pipe with rigid walls filled with micropolar fluid). Now, we try to construct the second-order corrector \hat{T}_2 . Plugging the expansion (7) into (5) and (6) and collecting $\mathfrak{O}(\varepsilon^2)$ terms, we get

$$\varepsilon^{2} : \frac{\partial \hat{T}_{0}}{\partial \hat{t}} + \frac{\Pr Re}{2} \left(\hat{u}_{0} \frac{\partial \hat{T}_{1}}{\partial \hat{r}} + \hat{w}_{0} \frac{\partial \hat{T}_{1}}{\partial \hat{z}} + \hat{u}_{1} \frac{\partial \hat{T}_{0}}{\partial \hat{r}} + \hat{w}_{1} \frac{\partial \hat{T}_{0}}{\partial \hat{z}} \right) \\
= \frac{\partial^{2} \hat{T}_{2}}{\partial \hat{r}^{2}} + \frac{1}{\hat{r}} \frac{\partial \hat{T}_{2}}{\partial \hat{r}} + \frac{\partial^{2} \hat{T}_{0}}{\partial \hat{z}^{2}}, \\
\varepsilon^{2} : \frac{\partial \hat{T}_{2}}{\partial \hat{r}} = -Nu\hat{T}_{1} \text{ for } \hat{r} = 1. \tag{14}$$

We recall that $\frac{\partial \hat{T}_0}{\partial \hat{r}} = 0$ and employ the expressions derived for the hydrodynamic part [see (19)–(20), Appendix], namely

$$\begin{split} \hat{u}_0 &= \frac{1}{16} (2\hat{r} - \hat{r}^3) \frac{\partial^2 \hat{p}_0}{\partial \hat{z}^2} = (2\hat{r} - \hat{r}^3) \hat{p}_0(\hat{z}), \\ \hat{w}_0 &= -\frac{1}{4} (1 - \hat{r}^2) \frac{\partial \hat{p}_0}{\partial \hat{z}}, \\ \hat{u}_1 &= \frac{1}{16} (2\hat{r} - \hat{r}^3) \frac{\partial^2 \hat{p}_1}{\partial \hat{z}^2} + \frac{1}{18432} (58\hat{r} - 36\hat{r}^3) \\ &\quad + 6\hat{r}^5 - \hat{r}^7) Re \left(\left(\frac{\partial^2 \hat{p}_0}{\partial \hat{z}^2} \right)^2 + \frac{\partial \hat{p}_0}{\partial \hat{z}} \frac{\partial^3 \hat{p}_0}{\partial \hat{z}^3} \right), \\ \hat{w}_1 &= -\frac{1}{4} (1 - \hat{r}^2) \frac{\partial \hat{p}_1}{\partial \hat{z}} - \frac{1}{4608} (29 - 36\hat{r}^2) \\ &\quad + 9\hat{r}^4 - 2\hat{r}^6) Re \frac{\partial^2 \hat{p}_0}{\partial \hat{z}^2} \frac{\partial \hat{p}_0}{\partial \hat{z}} \\ &= -\frac{1}{4} (1 - \hat{r}^2) \frac{\partial \hat{p}_1}{\partial \hat{z}} - \frac{1}{288} (29 - 36\hat{r}^2) \\ &\quad + 9\hat{r}^4 - 2\hat{r}^6) Re \hat{p}_0 \frac{\partial \hat{p}_0}{\partial \hat{z}}, \end{split}$$

$$\hat{p}_0 = -2 \sinh(4\hat{z}) + \hat{P}_{tm} \cosh(4\hat{z}),$$

$$\hat{p}_1 = \frac{Re}{8} (4 + \hat{P}_{tm}^2) (\cosh(4\hat{z}) - \cosh(8\hat{z}))$$

$$- \frac{Re\hat{P}_{tm}}{4} (\sinh(4\hat{z}) - 2 \sinh(8\hat{z})).$$

The compatibility condition for (14) yields

$$\begin{split} \pi \frac{\partial \hat{T}_0}{\partial \hat{t}} &- \pi \frac{\partial^2 \hat{T}_0}{\partial \hat{z}^2} + 2 \pi \frac{\text{PrRe}}{2} \\ & \left(\frac{\partial^2 \hat{p}_0}{\partial \hat{z}^2} \frac{1}{16} \text{Nu} (\hat{G} - \hat{T}_0) \int_0^1 (2\hat{r} - \hat{r}^3)^2 \hat{r} d\hat{r} \right) \\ &+ 2 \pi \frac{\text{PrRe}}{2} \left(-\frac{1}{4} \frac{\partial \hat{p}_0}{\partial \hat{z}} \text{Nu} \left(\frac{\partial \hat{G}}{\partial \hat{z}} - \frac{\partial \hat{T}_0}{\partial \hat{z}} \right) \int_0^1 (1 - \hat{r}^2) \right. \\ & \left. \left(\hat{r}^2 - \frac{\hat{r}^4}{4} \right) \hat{r} d\hat{r} - \frac{1}{4} \frac{\partial \hat{C}}{\partial \hat{z}} \frac{\partial \hat{p}_0}{\partial \hat{z}} \int_0^1 (1 - \hat{r}^2) \hat{r} d\hat{r} \right. \\ &+ 2 \pi \frac{\text{PrRe}}{2} \frac{\partial \hat{T}_0}{\partial \hat{z}} \left(-\frac{1}{4} \frac{\partial \hat{p}_1}{\partial \hat{z}} \int_0^1 (1 - \hat{r}^2) \hat{r} d\hat{r} \right. \\ & \left. - \frac{\text{Re}}{4608} \frac{\partial^2 \hat{p}_0}{\partial \hat{z}^2} \frac{\partial \hat{p}_0}{\partial \hat{z}} \int_0^1 (29 - 36\hat{r}^2 + 9\hat{r}^4 - 2\hat{r}^6) \hat{r} d\hat{r} \right. \\ &= -2 \pi \text{Nu} \left(\frac{3}{4} \text{Nu} (\hat{G} - \hat{T}_0) + \hat{C} \right). \end{split}$$

After integration, we obtain

$$\begin{split} \frac{\partial \hat{T}_0}{\partial \hat{t}} &- \frac{\partial^2 \hat{T}_0}{\partial \hat{z}^2} + \text{PrRe}\bigg(\frac{11}{384} \frac{\partial^2 \hat{p}_0}{\partial \hat{z}^2} Nu(\hat{G} - \hat{T}_0) \\ &- \frac{7}{384} \frac{\partial \hat{p}_0}{\partial \hat{z}} Nu \bigg(\frac{\partial \hat{G}}{\partial \hat{z}} - \frac{\partial \hat{T}_0}{\partial \hat{z}}\bigg) - \frac{1}{16} \frac{\partial \hat{p}_0}{\partial \hat{z}} \frac{\partial \hat{C}}{\partial \hat{z}}\bigg) \\ &+ \text{PrRe} \frac{\partial \hat{T}_0}{\partial \hat{z}} \bigg(-\frac{1}{16} \frac{\partial \hat{p}_1}{\partial \hat{z}} - \frac{3Re}{2048} \frac{\partial^2 \hat{p}_0}{\partial \hat{z}^2} \frac{\partial \hat{p}_0}{\partial \hat{z}}\bigg) \bigg) \\ &= -\frac{3}{2} Nu^2 (\hat{G} - \hat{T}_0) - 2Nu\hat{C}, \end{split}$$

implying

$$\frac{\text{PrRe}}{16} \frac{\partial \hat{p}_0}{\partial \hat{z}} \frac{\partial \hat{C}}{\partial \hat{z}} - 2Nu\hat{C} = \hat{D}(\hat{z}, \hat{t}), \tag{15}$$

where

$$\hat{D}(\hat{z}, \hat{t}) = \frac{\partial \hat{T}_0}{\partial \hat{t}} - \frac{\partial^2 \hat{T}_0}{\partial \hat{z}^2} + \frac{3}{2} N u^2 (\hat{G} - \hat{T}_0)
+ \text{PrRe} \left(\frac{11}{384} \frac{\partial^2 \hat{p}_0}{\partial \hat{z}^2} N u (\hat{G} - \hat{T}_0) \right)$$

$$+ \operatorname{PrRe} \left(-\frac{7}{384} \frac{\partial \hat{p}_0}{\partial \hat{z}} Nu \left(\frac{\partial \hat{G}}{\partial \hat{z}} - \frac{\partial \hat{T}_0}{\partial \hat{z}} \right) \right.$$
$$\left. - \frac{1}{16} \frac{\partial \hat{p}_1}{\partial \hat{z}} \frac{\partial \hat{T}_0}{\partial \hat{z}} - \frac{3Re}{2048} \frac{\partial^2 \hat{p}_0}{\partial \hat{z}^2} \frac{\partial \hat{p}_0}{\partial \hat{z}} \frac{\partial \hat{T}_0}{\partial \hat{z}} \right).$$

In view of (11), we rewrite (15) as

$$\frac{\partial \hat{C}}{\partial \hat{z}} - \frac{16Nu}{\text{PrRe}(\hat{P}_{tm} - 2)} \frac{e^{4\hat{z}}}{e^{8\hat{z}} - \frac{\hat{P}_{tm} + 2}{\hat{P}_{tm} - 2}} \hat{C} = \hat{E}(\hat{z}, \hat{t}), \quad (16)$$

with

$$\hat{E}(\hat{z},\hat{t}) = \frac{8}{\text{PrRe}(\hat{P}_{tm}-2)} \frac{e^{4\hat{z}}}{e^{8\hat{z}} - \frac{\hat{P}_{tm}+2}{\hat{P}_{tm}-2}} \hat{D}(\hat{z},\hat{t}).$$

For fixed time $\hat{t} \in (0, 1)$, we can solve (16) as an ODE with respect to z. We obtain

$$\hat{C}(\hat{z},\hat{t}) = \left(rac{e^{4\hat{z}} - \sqrt{rac{\hat{P}_{tm} + 2}{\hat{P}_{tm} - 2}}}{e^{4\hat{z}} + \sqrt{rac{\hat{P}_{tm} + 2}{\hat{P}_{tm} - 2}}}
ight)^{rac{2Nu}{ ext{PrRe}(\hat{P}_{tm} - 2)}} \sqrt{rac{1}{rac{\hat{P}_{tm} + 2}{\hat{P}_{tm} - 2}}} \ \int\limits_{0}^{\hat{z}} \hat{E}(\xi,\hat{t}) \left(rac{e^{4\hat{z}} - \sqrt{rac{\hat{P}_{tm} + 2}{\hat{P}_{tm} - 2}}}{e^{4\hat{z}} + \sqrt{rac{\hat{P}_{tm} + 2}{\hat{P}_{tm} - 2}}}
ight)^{-rac{2Nu}{ ext{PrRe}(\hat{P}_{tm} - 2)}} \sqrt{rac{1}{rac{\hat{P}_{tm} + 2}{\hat{P}_{tm} - 2}}} \ \mathrm{d}\xi,$$

where we took $\hat{C}(0,\hat{t}) = 0$. The problem (14) for the second-order corrector \hat{T}_2 now reads

$$\begin{split} \frac{\partial^2 \hat{T}_2}{\partial \hat{r}^2} &+ \frac{1}{\hat{r}} \frac{\partial \hat{T}_2}{\partial \hat{r}} \\ &= \frac{\partial \hat{T}_0}{\partial \hat{t}} - \frac{\partial^2 \hat{T}_0}{\partial \hat{z}^2} \\ &+ \frac{\text{PrRe}}{2} \hat{p}_0 (2\hat{r} - \hat{r}^3)^2 N u (\hat{G} - \hat{T}_0) \\ &- \frac{\text{PrRe}Nu}{8} (1 - \hat{r}^2) \left(\hat{r}^2 - \frac{\hat{r}^4}{4} \right) \frac{\partial \hat{p}_0}{\partial \hat{z}} \left(\frac{\partial \hat{G}}{\partial \hat{z}} - \frac{\partial \hat{T}_0}{\partial \hat{z}} \right) \\ &- \frac{\text{PrRe}}{8} (1 - \hat{r}^2) \frac{\partial \hat{p}_0}{\partial \hat{z}} \frac{\partial \hat{C}}{\partial \hat{z}} - \frac{\text{PrRe}}{8} (1 - \hat{r}^2) \frac{\partial \hat{p}_1}{\partial \hat{z}} \frac{\partial \hat{T}_0}{\partial \hat{z}} \\ &- \frac{\text{PrRe}^2}{576} (29 - 36\hat{r}^2 + 9\hat{r}^4 - 2\hat{r}^6) \hat{p}_0 \frac{\partial \hat{p}_0}{\partial \hat{z}} \frac{\partial \hat{T}_0}{\partial \hat{z}}, \\ \frac{\partial \hat{T}_2}{\partial \hat{r}} &= -Nu \, \hat{T}_1 \quad \text{for} \quad \hat{r} = 1. \end{split}$$

It can be verified that \hat{T}_2 is given by

$$\hat{T}_{2}(\hat{z}, \hat{r}, \hat{t})$$

$$= \frac{1}{4} \left(\frac{\partial \hat{T}_{0}}{\partial \hat{t}} - \frac{\partial^{2} \hat{T}_{0}}{\partial \hat{z}^{2}} \right) \hat{r}^{2}$$

$$+ \frac{\Pr{ReNu}}{2} \hat{p}_{0} (\hat{G} - \hat{T}_{0}) \left(\frac{\hat{r}^{8}}{64} - \frac{\hat{r}^{6}}{9} + \frac{\hat{r}^{4}}{4} \right)$$

$$- \frac{\Pr{ReNu}}{8} \frac{\partial \hat{p}_{0}}{\partial \hat{z}} \left(\frac{\partial \hat{G}}{\partial \hat{z}} - \frac{\partial \hat{T}_{0}}{\partial \hat{z}} \right) \left(\frac{\hat{r}^{8}}{256} - \frac{5\hat{r}^{6}}{144} + \frac{\hat{r}^{4}}{16} \right)$$

$$- \frac{\Pr{Re}}{8} \frac{\partial \hat{p}_{0}}{\partial \hat{z}} \frac{\partial \hat{C}}{\partial \hat{z}} \left(\frac{\hat{r}^{2}}{4} - \frac{\hat{r}^{4}}{16} \right)$$

$$- \frac{\Pr{Re}}{8} \frac{\partial \hat{p}_{1}}{\partial \hat{z}} \frac{\partial \hat{T}_{0}}{\partial \hat{z}} \left(\frac{\hat{r}^{2}}{4} - \frac{\hat{r}^{4}}{16} \right)$$

$$- \frac{\Pr{Re}^{2}}{576} \hat{p}_{0} \frac{\partial \hat{p}_{0}}{\partial \hat{z}} \frac{\partial \hat{T}_{0}}{\partial \hat{z}} \left(\frac{29\hat{r}^{2}}{4} - \frac{9\hat{r}^{4}}{4} + \frac{\hat{r}^{6}}{4} - \frac{\hat{r}^{8}}{32} \right).$$
(17)

This completes the construction of our approximate solution. To conclude this section, let us denote by $\hat{T}_{[0]}^{por} =$ \hat{T}_0 the zero-order approximation, while we use the following notation for the first- and second-order approximation:

$$egin{aligned} \hat{T}^{por}_{[1]}(\hat{z},\hat{r},\hat{t}) &= \hat{T}_0(\hat{z},\hat{t}) + \varepsilon \hat{T}_1(\hat{z},\hat{r},\hat{t}) \\ \hat{T}^{por}_{[2]}(\hat{z},\hat{r},\hat{t}) &= \hat{T}_0(\hat{z},\hat{t}) + \varepsilon \hat{T}_1(\hat{z},\hat{r},\hat{t}) + \varepsilon^2 \hat{T}_2(\hat{z},\hat{r},\hat{t}). \end{aligned}$$

It should be emphasised that the functions \hat{T}_0 , \hat{T}_1 , \hat{T}_2 are all provided in explicit form [see (12), (10), and (17), respectively]. This enables us to directly compare our results with the corresponding one derived for the tube with non-permeable, rigid walls. Moreover, we can observe and notice the corrections coming due to the higher-order terms in the asymptotic solution. We address these issues in the forthcoming section by providing numerical examples.

4 Numerical Examples

Let us first derive the approximation for the tube with rigid walls. This essentially means that, instead of

$$w=0$$
, $u=\frac{k_m}{\mu h}p$ for $r=R$,

we consider the no-slip condition for both velocity components, namely w = u = 0 for r = R. As a result, we obtain a classical Poiseuille solution, which, in non-dimensional form, reads as follows:

$$\hat{w}_0^{rig} = \hat{w}_0^{rig}(\hat{r}) = -\frac{1}{4}(1-\hat{r}^2)\frac{\partial \hat{p}_0^{rig}}{\partial \hat{z}}, \quad \hat{u}_0^{rig} = 0.$$

Here, $-\frac{\partial \hat{p}_0^{\text{ng}}}{\partial \hat{z}} = Q$ is a positive constant. We now obtain

$$\frac{\partial \hat{T}_0^{\text{rig}}}{\partial \hat{z}} + \frac{32Nu}{\text{PrRe}Q} \hat{T}_0^{\text{rig}} = \frac{32Nu}{\text{PrRe}Q} \hat{G}(\hat{z}, \hat{t}),$$

leading to

$$\hat{T}_{[0]}^{\text{rig}}(\hat{z},\hat{t}) = e^{-\frac{32Nu}{\text{PrRe}Q}\hat{z}}(\hat{\theta}_{0}(\hat{t}) + \frac{32Nu}{\text{PrRe}Q}\int_{0}^{\hat{z}} e^{\frac{32Nu}{\text{PrRe}Q}}\hat{G}(\hat{\xi},\hat{t})d\hat{\xi}).$$
(18)

In the following numerical examples, we take the pressure drop Q = 41; the external and boundary temperatures are assumed to be constant, namely $\hat{G}=10$ and

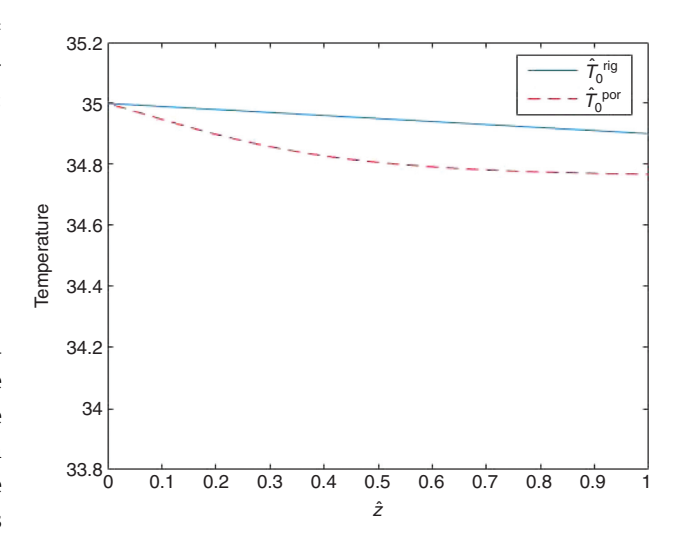


Figure 2: Comparison of zero-order approximations $\hat{T}_{[0]}^{\text{rig}}$ and $\hat{T}_{[0]}^{\text{por}}$.

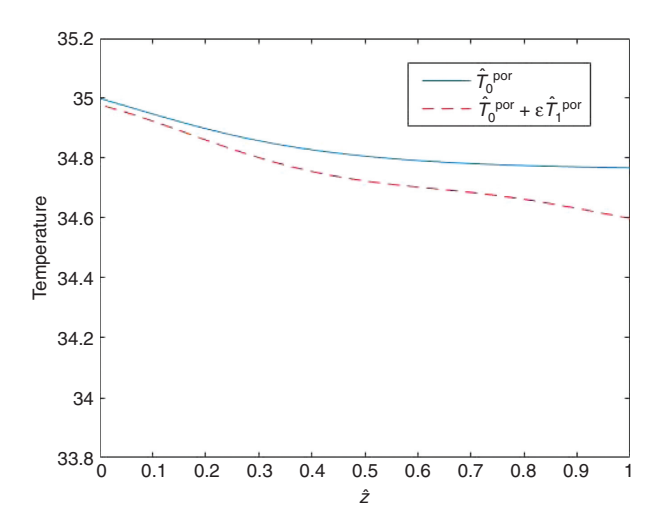


Figure 3: Comparison of zero-order approximation $\hat{\mathcal{T}}^{por}_{[0]}$ and first-order asymptotic approximation $\hat{\mathcal{T}}^{por}_{[1]}$ for fixed $\hat{r}=0.5$.

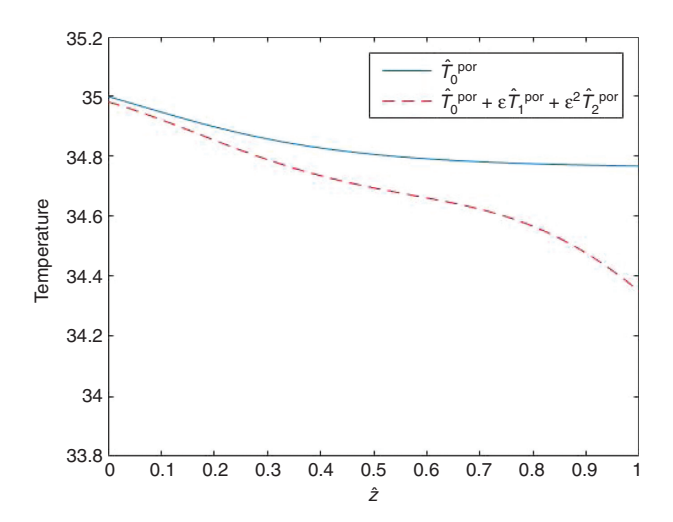


Figure 4: Comparison of zero-order approximation $\hat{T}^{por}_{[0]}$ with the second-order asymptotic approximation $\hat{T}^{por}_{[2]}$ for fixed $\hat{r}=$ 0.5.

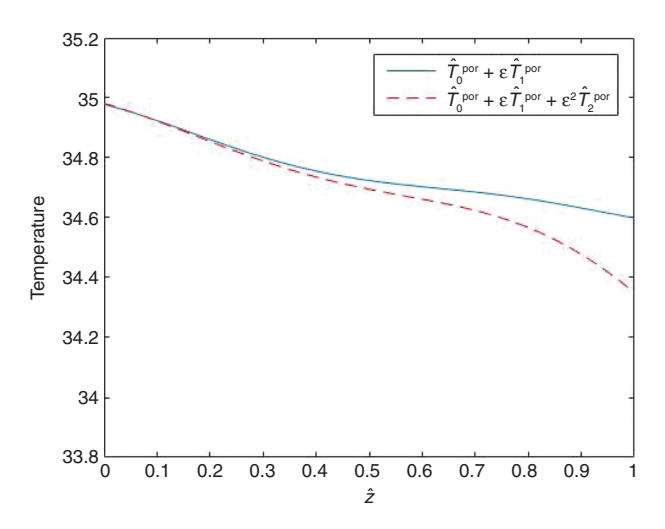


Figure 5: Comparison of first-order asymptotic approximation $\hat{T}^{\text{por}}_{[1]}$ with the second-order asymptotic approximation $\hat{T}^{\text{por}}_{[2]}$ for fixed $\hat{r}=0.5$.

 $\hat{\theta}_0=35$ (see, e.g. [2]). The characteristic numbers take the following values: Nu=3.66, Pr=4.8, Re=150. The non-dimensional transmembrane pressure at z=0 is set to $\hat{P}_{tm}=0.5$. The small parameter is taken as $\varepsilon=10^{-3}$. It should be mentioned that the small parameter ε is usually linked with the non-dimensional permeability of the system σ as $\varepsilon=\sqrt{\sigma}$, so this means that we are considering the so-called microfiltration systems (see [1] for details).

Taking into account the above data, we first compare the zero-order approximations $\hat{T}^{\rm rig}_{[0]}$ and $\hat{T}^{\rm por}_{[0]}$ (see Fig. 2). Next, we focus solely on the porous tube and plot the first-order asymptotic approximation $\hat{T}^{\rm por}_{[1]}$ for a fixed parameter $\hat{r}=0.5$ and compare it with the zero-order approximation

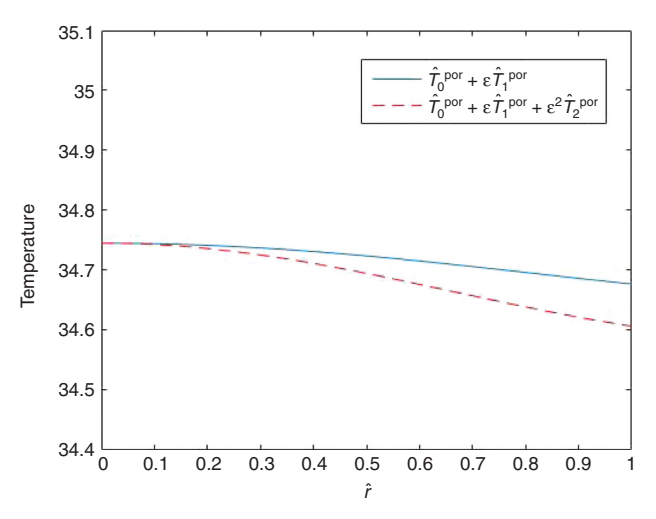


Figure 6: Comparison of first-order asymptotic approximation $\hat{T}^{\text{pot}}_{[1]}$ with the second-order asymptotic approximation $\hat{T}^{\text{por}}_{[2]}$ for fixed $\hat{z}=0.5$.

 $\hat{T}_{[0]}^{
m por}$ (see Fig. 3). Finally, we compare $\hat{T}_{[0]}^{
m por}$ and $\hat{T}_{[1]}^{
m por}$ with the second-order asymptotic approximation $\hat{T}_{[2]}^{
m por}$ for fixed parameters $\hat{r}=0.5$ and $\hat{z}=0.5$ (see Figs. 4–6).

5 Conclusions

In Section 3, a second-order asymptotic model describing the heat transfer in a porous tube has been proposed, where the zero-order approximation and the first- and second-order correctors for the temperature have been explicitly computed. Section 4 is devoted to visualisations based on our analytical results. Let us mention that we have taken the small parameter $\varepsilon = 10^{-3}$ and Reynolds number Re = 150 in order to be consistent with the discussion provided in [1].

Comparing the zero-order approximations $\hat{T}_{[0]}^{\mathrm{rig}}$ and $\hat{T}_{[0]}^{\mathrm{por}}$ derived for the case of a rigid and porous tube, respectively (see Fig. 2), we observe that the temperature drop is greater in the porous case, as we move along the tube. The physical explanation for this far-field behaviour is that, moving along the tube in the axial direction, there is additional temperature loss through the porous boundary in the case of the tube with permeable walls as opposed to the case with a tube with rigid walls, where this additional loss of temperature does not take place and we have cooling only due to the difference between the exterior temperature and the temperature of the fluid.

A comparison of the zero-order approximation $\hat{T}^{\rm por}_{[0]}$ for a porous tube with the first- and second-order asymptotic approximations, $\hat{T}^{\rm por}_{[1]}$ and $\hat{T}^{\rm por}_{[2]}$ (for fixed $\hat{r}=0.5$), clearly indicates the effects of the higher-order terms as \hat{z}

increases (see Figs. 3 and 4). As expected, those effects are more noticeable for the second-order solution $\hat{T}_{[2]}$.

Finally, comparing the first- and second-order asymptotic solutions $\hat{T}_{[1]}^{\text{por}}$ and $\hat{T}_{[2]}^{\text{por}}$ for fixed $\hat{r}=0.5$ and $\hat{z}=0.5$, we see that the second-order approximation $\hat{T}_{[2]}^{\mathrm{por}}$ shows a greater temperature drop as \hat{z} and \hat{r} increase (see Figs. 5 and 6).

Again, as we are considering a tube with permeable walls, the first- and second-order temperature correctors \hat{T}_1^{por} and \hat{T}_2^{por} give a more precise approximation of the effects of additional temperature loss due to porosity of the boundary as we move along the tube and near its lateral boundary, which was to be expected.

A natural extension of the results presented in this paper would be to take additional physical effects into consideration. Analytical studies of the magnetohydrodynamic natural convection flow occurring about a heated vertically stretching permeable surface placed in a saturated porous media under the influence of a temperaturedependent internal heat generation or absorption, as well as the magnetohydrodynamic slip flow and heat transfer of stagnation point Jeffrey fluid over deformable surfaces, were recently considered in [25] and [26]. Taking these results into account, a possible direction for future work would be to derive a lower-dimensional model for the magnetohydrodynamic flow and heat transfer in a porous tube setting using the two-scale expansion technique employed in the derivation of the model in this paper.

Finally, we refer the reader to the work presented in [2], where an asymptotic model was derived for the heat flow through a thin cooled pipe with rigid walls filled with micropolar fluid with numerical illustration provided, where one can clearly see the effects of enhanced cooling as the result of the micropolarity of the fluid. Motivated by this result, we can consider the heat flow through a porous tube filled with micropolar fluid and consider the effects of the micropolarity of the fluid in this setting as an additional possibility for future work.

Acknowledgements: The first author of this work has been supported by the Croatian Science Foundation (scientific project: Multiscale Problems in Fluid Mechanics -MultiFM). The second author of this work has been supported by the Croatian Science Foundation (scientific project: Asymptotic Analysis of the Boundary Value Problems in Continuum Mechanics - AsAn). The authors would like to thank the referees for their helpful comments and suggestions that helped improve the paper.

Appendix: Approximation for the **Hvdrodvnamic Part**

In this appendix, for the reader's convenience, we recover the results from [1] concerning the hydrodynamic part of our problem.

A steady, axisymmetric, incompressible fluid flow in Ω is considered, where the fluid region outside the tube is maintained at a constant uniform pressure P_{ref} (P_{ref} = 0, without loss of generality). An axial pressure gradient drives an axial Poiseuille flow w, while the transmembrane pressure difference drives radial suction or injection u. In view of that, the fluid flow equations in cylindrical coordinates read as follows:

$$\begin{split} u\frac{\partial u}{\partial r} + w\frac{\partial u}{\partial z} + \frac{1}{\rho}\frac{\partial p}{\partial r} \\ &- \frac{\mu}{\rho} \left(\frac{\partial^2 u}{\partial r^2} + \frac{1}{r}\frac{\partial u}{\partial r} - \frac{u}{r^2} + \frac{\partial^2 u}{\partial z^2} \right) = 0, \\ u\frac{\partial w}{\partial r} + w\frac{\partial w}{\partial z} + \frac{1}{\rho}\frac{\partial p}{\partial z} \\ &- \frac{\mu}{\rho} \left(\frac{\partial^2 w}{\partial r^2} + \frac{1}{r}\frac{\partial w}{\partial r} + \frac{\partial^2 w}{\partial z^2} \right) = 0, \\ \frac{\partial u}{\partial r} + \frac{u}{r} + \frac{\partial w}{\partial z} = 0, \end{split}$$

where p is the fluid pressure and μ represents the dynamic viscosity of the fluid. The boundary conditions on the permeable surface are given by the standard no-slip condition and Darcy's law:

$$w = 0$$
, $u = \frac{k_m}{uh}p$ for $r = R$,

where k_m denotes the permeability of the membrane, while h represents its thickness. To solve the problem, the transmembrane pressure and mean axial velocity at z=0are prescribed:

$$P_{tm}=p|_{r=R}, \quad \overline{w}_0=rac{1}{\pi R^2}\int\limits_0^R 2\pi w r \mathrm{d}r \quad ext{for} \quad z=0.$$

The problem is rewritten in non-dimensional form by introducing

$$\hat{z} = rac{z}{L}, \quad \hat{r} = rac{r}{R}, \quad \hat{u} = rac{u}{arepsilon \overline{w}_0},$$
 $\hat{w} = rac{w}{\overline{w}_0}, \quad \hat{p} = rac{arepsilon R}{u \overline{w}_0} p.$

Linking the small parameter $\varepsilon = \frac{R}{I}$ with the nondimensional permeability $\sigma = \frac{k_m}{hR}$ as $\varepsilon = \sqrt{\sigma}$, we get

$$\begin{split} \varepsilon^3 \hat{u} \frac{\partial \hat{u}}{\partial \hat{r}} + \varepsilon^3 \hat{w} \frac{\partial \hat{u}}{\partial \hat{z}} + \frac{2}{Re} \frac{\partial \hat{p}}{\partial \hat{r}} \\ - \frac{2\varepsilon^2}{Re} \left(\frac{\partial^2 \hat{u}}{\partial \hat{r}^2} + \frac{1}{\hat{r}} \frac{\partial \hat{u}}{\partial \hat{r}} - \frac{\hat{u}}{\hat{r}^2} + \varepsilon^2 \frac{\partial^2 \hat{u}}{\partial \hat{z}^2} \right) = 0, \\ \varepsilon \hat{u} \frac{\partial \hat{w}}{\partial \hat{r}} + \varepsilon \hat{w} \frac{\partial \hat{w}}{\partial \hat{z}} + \frac{2}{Re} \frac{\partial \hat{p}}{\partial \hat{z}} \\ - \frac{2}{Re} \left(\frac{\partial^2 \hat{w}}{\partial \hat{r}^2} + \frac{1}{\hat{r}} \frac{\partial \hat{w}}{\partial \hat{r}} + \varepsilon^2 \frac{\partial^2 \hat{w}}{\partial \hat{z}^2} \right) = 0, \\ \frac{\partial \hat{u}}{\partial \hat{r}} + \frac{\hat{u}}{\hat{r}} + \frac{\partial \hat{w}}{\partial \hat{z}} = 0, \\ \hat{w} = 0, \quad \hat{u} = \hat{p} \quad \text{for} \quad \hat{r} = 1, \\ \hat{p}|_{\hat{r}=1} = \hat{P}_{tm}, \quad \overline{\hat{w}} = 1 \quad \text{for} \quad \hat{z} = 0, \end{split}$$

where $\hat{P}_{tm}=rac{\varepsilon RP_{tm}}{\mu\overline{w}_0}$ is the non-dimensional transmembrane pressure at $\hat{z}=0$.

Expanding the unknown velocity and pressure as

$$\hat{w}(\hat{z},\hat{r}) = \hat{w}_0(\hat{z},\hat{r}) + \varepsilon \hat{w}_1(\hat{z},\hat{r}) + \cdots,$$
 $\hat{u}(\hat{z},\hat{r}) = \hat{u}_0(\hat{z},\hat{r}) + \varepsilon \hat{u}_1(\hat{z},\hat{r}) + \cdots,$ $\hat{p}(\hat{z}) = \hat{p}_0(\hat{z}) + \varepsilon \hat{p}_1(\hat{z}) + \cdots.$

and substituting it into the above system, the zero-order approximation takes the following form:

$$\begin{split} \hat{w}_{0}(\hat{z},\hat{r}) &= -\frac{1}{4}(1-\hat{r}^{2})\frac{\partial\hat{p}_{0}}{\partial\hat{z}},\\ \hat{u}_{0}(\hat{z},\hat{r}) &= \frac{1}{16}(2\hat{r}-\hat{r}^{3})\frac{\partial^{2}\hat{p}_{0}}{\partial\hat{z}},\\ \hat{p}_{0}(\hat{z}) &= -2\sinh(4\hat{z}) + \hat{P}_{tm}\cosh(4\hat{z}). \end{split} \tag{19}$$

Collecting the $\mathcal{O}(\varepsilon)$ terms yields the first-order corrector:

$$\hat{w}_{1}(\hat{z},\hat{r}) = -\frac{1}{4}(1-\hat{r}^{2})\frac{\partial\hat{p}_{1}}{\partial\hat{z}} - \frac{Re}{4608}(29-36\hat{r}^{2}) + 9\hat{r}^{4} - 2\hat{r}^{6}\frac{\partial^{2}\hat{p}_{0}}{\partial\hat{z}^{2}}\frac{\partial\hat{p}_{0}}{\partial\hat{z}},$$

$$\hat{u}_{1}(\hat{z},\hat{r}) = \frac{1}{16}(2\hat{r}-\hat{r}^{3})\frac{\partial^{2}\hat{p}_{1}}{\partial\hat{z}^{2}} + \frac{Re}{18432}(58\hat{r}-36\hat{r}^{3}+6\hat{r}^{5}-\hat{r}^{7})$$

$$\left(\left(\frac{\partial^{2}\hat{p}_{0}}{\partial\hat{z}^{2}}\right)^{2} + \frac{\partial\hat{p}_{0}}{\partial\hat{z}}\frac{\partial^{3}\hat{p}_{0}}{\partial\hat{z}^{3}}\right),$$

$$\hat{p}_{1}(\hat{z}) = \frac{Re}{8} (4 + \hat{P}_{tm}^{2})(\cosh(4\hat{z}) - \cosh(8\hat{z}))$$
$$-\frac{Re\hat{P}_{tm}}{4}(\sinh(4\hat{z}) - 2\sinh(8\hat{z})). \quad (20)$$

The computation details can be found in [1].

Nomenclature

circular tube with permeable walls length of the tube Ω R radius of the tube $\boldsymbol{\Omega}$ ratio of R and Laxial component of the velocity field radial component of the velocity field fluid pressure fluid temperature radius variable longitudinal variable time variable permeability of the membrane thickness of the membrane dynamic viscosity exterior temperature \overline{w}_0 mean axial velocity at z = 0transmembrane pressure at z=0kinematic viscosity Q pressure drop C_p kspecific heat capacity thermal conductivity β heat transfer coefficient fluid density non-dimensional axial component of the velocity field non-dimensional radial component of the velocity field р Т non-dimensional fluid pressure non-dimensional fluid temperature î non-dimensional radius variable non-dimensional longitudinal variable î non-dimensional time variable Re Revnolds number Pr Prandtl number Nu Nusselt number Ĝ non-dimensional exterior temperature characteristic temperature T_{ref} \hat{P}_{tm} non-dimensional transmembrane pressure at $\hat{z}=0$ $T_{\rm ref}$ pressure of the fluid region outside the tube

References

[1] N. Tilton, D. Martinard, E. Serre, and R. M. Lueptow, AIChE J. 58, 2030 (2012).

non-dimensional permeability

- M. Beneš, I. Pažanin, and F. J. Suarez-Grau, J. Theor. Appl. Mech. 53, 569 (2015).
- S. Marušić, E. Marušić-Paloka, and I. Pažanin, C.R. Mécanique 336, 493 (2008).
- [4] E. Marušić-Paloka and I. Pažanin, Appl. Anal. 88, 495
- [5] E. Marušić-Paloka and I. Pažanin, Math. Comput. Model. 50, 1571 (2009).

- [6] E. Marušić-Paloka and I. Pažanin, Nonlinear Anal. RWA 11, 4554
- [7] A. S. Berman, J. Appl. Phys. 24, 1232 (1953).
- [8] S. A. Regirer, Sov. Phys. Tech. Phys. 5, 602 (1960).
- [9] M. E. Ali, Int. J. Therm. Sci. 46, 157 (2007).
- [10] I. Borsi, A. Farina, and A. Fasano, Z. Angew. Math. Phys. 62, 681 (2011).
- [11] P. Haldenwang, J. Fluid Mech. **593**, 463 (2007).
- [12] W. Jäger and A. Mikelić, Transp. Porous Med. 78, 489 (2009).
- [13] S. K. Karode, J. Membr. Sci. 191, 237 (2001).
- [14] A. S. Kim and Y. T. Lee, AlChE J. 57 (2011), https://doi.org/10. 1002/aic.12430.
- [15] S. J. Mamouri, V. V. Tarabara, and A. Benard, J. Membr. Sci. **523**, 373 (2017).
- [16] Y. Moussy and A. D. Snider, J. Membr. Sci. 327, 104 (2009).

- [17] A. I. Alsabery, H. Saleh, I. Hashim, and P. G. Siddheshwar, Int. J. Mech. Sci. 114, 233 (2016).
- [18] A. Barletta, J. Fluid Mech. 770, 273 (2015).
- [19] W. Chen and W. Liu, Appl. Therm. Eng. 28, 1251 (2008).
- [20] Y. C. Cheng and G. J. Wang, Int. J. Heat Mass Transf. 38, 3475 (1995).
- [21] S. Ferro and G. Gnavi, Phys. Fluids 14, 839 (2002).
- [22] D. A. S. Rees, Trans. Porous Med. 87, 459 (2011).
- [23] N. L. Scott and B. Straughan, J. Math. Fluid Mech. 15, 171 (2013).
- [24] O. A. Ladyzhenskaya, V. A. Solonnikov, and N. N. Uraltseva, Translations of Mathematical Monographs Vol. 23, American Mathematical Society, Providence, RI 1967.
- [25] M. Turkyilmazoglu, Arch. Mech. 71, 49 (2019).
- [26] M. Turkyilmazoglu, Z. Naturforsch. A 71, 549 (2016).